

Physiological significance of Rag1 in neuronal death, especially optic neuropathy

Takao Hirano, Toshinori Murata¹, Takuma Hayashi²

¹Department of Ophthalmology, Shinshu University Graduate School of Medicine,
3-1-1 Asahi, Matsumoto, Nagano 390-8621, Japan

²Department of Immunology and Infectious Disease, Shinshu University Graduate School of
Medicine, 3-1-1 Asahi, Matsumoto, Nagano 390-8621, Japan

Correspondence

Takuma Hayashi

Department of Immunology and Infectious Disease, Shinshu University Graduate School of
Medicine,

3-1-1 Asahi, Matsumoto, Nagano 390-8621, Japan;

Phone: +81-263-37-2611;

email: takumah@shinshu-u.ac.jp

Running title

Rag1 is involved in retinal ganglion cell death

Abbreviations

NF- κ B, nuclear factor-kappa B; CNS, central nervous system; NMDA, N-methyl-D-aspartate ;
RGCs, retinal ganglion cells; Rag, recombination activating gene; H.E., hematoxylin and eosin
staining; IHC, immunohistochemistry; IOP, intraocular pressure; GCL, ganglion cell layer

Key words

Rag1, NF- κ Bp50, programmed cell death, RGCs, optic neuropathy

Abstract

Although the transcription factor NF- κ B is known to regulate cell death and survival, its precise role in cell death within the central nervous system remains unknown. We previously reported that mice with a homozygous deficiency for NF- κ Bp50 spontaneously develop optic neuropathy. The aim of the present study was to demonstrate the expression and activation of pro-apoptotic factor(s), which mediate optic neuropathy in p50-deficient mice. Recombination-activating gene 1 (Rag1) is known to activate the recombination of immunoglobulin V(D)J. In this study, experiments with genetically-engineered mice revealed the involvement of Rag1 expression in apoptosis of Brn3a positive retinal ganglion cells (RGCs), and also demonstrated the specific effect of p50-deficiency on the activation of *Rag1* gene transcription. Furthermore, genetic analysis of murine neuronal stem-like cells clarified the biological significance of Rag1 in NMDA-induced neuronal apoptosis. We also detected the apoptotic regulating factors, Bax, and cleaved caspase 3, 8, and 9 in HEK293 cells expressing external molecule of Rag1, and a human histological examination revealed the expression of Rag1 in RGCs. The result of the present study indicated that Rag1 played a role in optic neuropathy as a pro-apoptotic candidate in p50-deficient mice. This result may lead to new therapeutic targets in optic neuropathy.

Introduction

As a transcriptional factor, nuclear factor-kappa B (NF- κ B) plays a key role in cell survival or death signaling pathways, acute central nervous system (CNS) trauma, and chronic neurodegenerative disorders [1,2]. The NF- κ B family, which is primarily composed of p50/p65 (RelA) heterodimers, has been detected in almost animal cell types and is involved in cellular responses to stimuli such as stress and cytokines [3]. NF- κ B is sequestered in the cytoplasm of unstimulated cells by a class of inhibitors called I κ Bs. The degradation of I κ B allows NF- κ B to enter the nucleus, in which it specifically initiates the expression of target genes. Accordingly, the impaired regulation of NF- κ B has been linked to various diseases, including cancer, inflammatory disorders, and autoimmune diseases, as well as deficiencies in the processes of synaptic plasticity and memory [4]. Activated

NF- κ Bp65 has been suggested to glutamate-induced neurotoxicity, N-methyl-D-aspartate (NMDA)-induced retinal neuronal cell death, retinal ischemia, and reperfusion injury in the CNS [5-8]. We previously reported that the number of retinal ganglion cells (RGCs) in p50-deficient ($p50^{-/-}$) mice was significantly lower than that in $p50^{+/+}$ mice, suggesting that these animals exhibited features resembling those of human glaucoma [9]. However, the precise role of NF- κ B in cell death within the CNS remains controversial.

Verkoczy L *et al.* reported that NF- κ B was relevant in the B-cell receptor-mediated regulation of recombination activating gene (Rag) locus transcription [10]. They suggested that immediately activated NF- κ B pathways may facilitate quick antigen receptor-regulated changes in Rag expression, which is important for editing [10]. *Rag* genes encode two enzymes that play key roles in the adaptive immune system: both Rag1 and Rag2 mediate the recombination of V(D)J, a process that is essential for the maturation of B and T cells [11]. Although previous studies have focused on the expression of Rag1 in the CNS, its role in CNS function is still unclear [12-14]. Chun JJ *et al.* demonstrated that Rag1 was present in the murine CNS, particularly in areas of high neural density, such as the cerebellum and hippocampal formation [12]. They suggested that Rag1 may function in neurons to site-specifically recombine elements of the neuronal genome or prevent detrimental alternations in the genomes of long-lived cells.

We hypothesized that Rag1 may exist in the visual system and play a role in programmed cell death. We first confirmed the presence of Rag1, but not Rag2 transcript in the eye. The absence of *Rag1* in $p50^{-/-}$ mice resulted in a decrease in optic nerve neuropathy. Along with several supporting lines of evidence, these results led us to the conclusion that Rag1 played a role in the programmed cell death of RGCs which was accelerated by NF- κ B, in p50-deficient mice. A protein homology study revealed that the human Rag1 molecule was 90% homologous with its mouse ortholog, suggesting that the physiological significance of Rag1 observed in mice may extend to regulation of human RGC survival.

Results

Rag1 expression in RGCs

We previously reported that the number of RGCs in $p50^{-/-}$ mice was significantly lower than that in littermate $p50^{+/+}$ mice, suggesting that these animals exhibited features resembling those found in human glaucoma [9]. The aim of the present study was to identify and clarify the molecular mechanism underlying RGC apoptosis in $p50^{-/-}$ mice. Molecules specifically expressed within the neurocyte may contribute to apoptosis and neuropathy. Although Rag1 generally plays an important role in the rearrangement and recombination of genes in immune cells for host defense, previous studies demonstrated the presence of Rag1 in the CNS. Since the expression and biological function of Rag1 in the retina have not yet been reported, we performed immunohistochemistry (IHC), Western blot analysis, and PCR experiments on retina tissues obtained from 6-month-old $p50^{+/+}$ mice. IHC revealed the expression of Rag1 but not Rag2 in the cytoplasm of ganglion cell layer (GCL) cells (Fig. 1A). Similar to the findings of previous reports, both Rag1 and Rag2 were present in lymphocytes [15] and Rag1 was only visible in the hippocampus [12] (Fig. 1A). Neither Rag1 nor Rag2 were detectable in the optic nerve (Fig. 1B). Because RGCs specially express Brn3, and constitute approximately 40-60% of neurons in the GCL of the mouse retina, with approximately half of these cells being amacrine cells, Rag1 was detected in the cytoplasm of cells positively stained for Brn3a, which has a role in dendritic- and cell soma-related stratification of RGCs [16, 17] (Fig. 1C). The normal rabbit IgG used in IHC did not reveal any significant findings, suggesting that Rag1 was specifically expressed in the cytoplasm of RGCs. Western blot analysis with anti-Rag1 antibody showed the expression of Rag1 in retinal crude extracts derived from both $p50^{+/+}$ and $p50^{-/-}$ mice (Fig. 1D). The expression of Rag1 in the retina was significantly higher in $p50^{-/-}$ mice than in wild type mice (Fig. 1D, E). A positive regulator of the NF- κ B family, such as RelA/cRel, may have mildly induced the expression of Rag1 in $p50^{-/-}$ mice. As indicated in previous studies, *Rag1* mRNA was strongly detected in both bone marrow and thymus specimens isolated from $p50^{+/+}$ mice [12]. Although *Rag1* mRNA was faintly detected by RT-PCR in RGCs purified using microbead-conjugated anti-mouse CD90.2 antibodies, it was clearly identified in pan-purified RGCs by nested-PCR (Fig. 1F). In contrast, we could not detect *Rag1* mRNA in other retinal cells. These results indicated that Rag1 was present specifically in RGCs.

Effects of Rag1 knockdown on the progressive loss of RGCs in p50-deficient mice

We next verified the reported age-related reduction in GCL cell number in $p50^{-/-}$ mice. The number of cells in the GCL was significantly lower in $p50^{-/-}$ mice than in $p50^{+/+}$ mice at both 6 and 15 months of age (Fig. 2A, B). To determine whether Rag1 played a biological role in various physiological mechanisms in the retina, we produced $p50^{-/-}Rag1^{-/-}$ double deficient mice by mating $p50^{-/-}$ mice with $Rag1^{-/-}$ mice. A histological examination showed that the retinas of $Rag1^{-/-}$ mice and $p50^{-/-}Rag1^{-/-}$ mice at 6 months of age were normal and indistinguishable from those of $p50^{+/+}$ mice (Fig. 2C). At 15 months, no significant differences were observed in the thickness or construction of any retinal layer, particularly the inner and outer nuclear layers (Fig. 2A). A closer examination showed no significant difference in GCL cell number between $p50^{-/-}Rag1^{-/-}$ mice and $p50^{+/+}$ mice. The GCL cell number was significantly higher in $p50^{-/-}Rag1^{-/-}$ mice than that in $p50^{-/-}$ mice (Fig. 2D). The quantification of Brn3-positive cells, which indicate RGCs revealed similar results among the four groups (Fig. 2E, F). We subsequently investigated the integrity of RGCs by retrograde labeling with Fluoro-Gold. The number of labeled RGCs after 7 days of retrograde transport was significantly lower in 6-month-old $p50^{-/-}$ mice than in $p50^{+/+}$ mice. This reduction was not observed in $p50^{-/-}Rag1^{-/-}$ mice, which was consistent with our histological findings (Fig. 2G, H). To investigate whether the decrease in live RGCs in $p50^{-/-}$ mice was attributable to cell death by apoptotic signaling, we carried out flow cytometric analysis with Annexin V staining. The numbers of early and late apoptotic cells among CD90.2 positive RGCs were significantly higher in $p50^{-/-}$ mice than in $p50^{+/+}$ mice. Furthermore, apoptotic cell counts were significantly lower in $p50^{-/-}Rag1^{-/-}$ mice than $p50^{-/-}$ mice (Fig. 2I, J). These results indicated that Rag1 played a key role in apoptotic signaling in the RGCs of $p50^{-/-}$ mice.

RGC axon degeneration is a hallmark of glaucoma, we therefore evaluated glaucomatous changes by quantifying axon densities in optic nerve cross-section specimens from the $p50^{+/+}$, $p50^{-/-}$, $p50^{-/-}Rag1^{-/-}$, and $Rag1^{-/-}$ mouse groups. Unlike our results for RGCs, no major structural changes and no significant differences were observed in optic nerve areas among the four groups examined

(Fig. 3A, B). Furthermore, no remarkable differences were noted regarding RGC axon density. However, axon degeneration was more frequently observed in the *p50*^{-/-} mouse group (Fig. 3C, D, E). These results suggested that RGC degeneration may have occurred in the retina due to a *p50* deficiency. In human glaucoma, RGC death is often caused by elevated intraocular pressure (IOP) and/or angle closure of the anterior chamber. No marked differences in IOP or no notable structural changes were observed in each of the 6-month-old mouse groups (Fig. 3F, G). Thus, increased IOP and angle closure of anterior chamber angle did not appear to be involved in RGC degeneration in the present.

Physiological function of Rag1 involved susceptibility to NMDA-induced neurotoxicity in *p50*^{-/-} mice

NMDA receptor-mediated cytotoxicity is known to contribute to glaucomatous neuropathy [18], whereby marked cell death has been observed in the retina of *p50*^{-/-} mice treated with a low-dose intravitreal injection of 5 nmol NMDA for 24h, however, this effect was not observed in *p50*^{+/+} mice. Therefore, we examined the expression of *Rag1* during NMDA-induced neurotoxicity in 4-month-old *p50*^{-/-} mice that had not yet exhibited optic neuropathy. A histological examination of retinas 24h after an intravitreal injection of 5 nmol NMDA showed a greater decrease in the number of RGCs in *p50*^{-/-} mice than in *p50*^{+/+} mice, as we reported previously [9]. However, no significant difference was observed between *p50*^{+/+} mice and *p50*^{-/-}*Rag1*^{-/-} mice (Fig. 4A). That treatment with NMDA induced cell death in the GCL more in *p50*^{-/-} mice than in *p50*^{-/-}*Rag1*^{-/-} mice (Fig. 4B). Thus, NMDA-induced neurotoxicity observed in the retina of *p50*^{-/-} mice appeared to be significantly prevented under Rag1-deficient cellular condition. These results suggested that NMDA-mediated neuronal cell death signaling involved the physiological function of Rag1.

Rag1 mediates cell death in vitro

To validate the physiological function of Rag1 on NMDA-induced neuronal cell death, *in vitro* experiments were performed using mouse neuronal stem-like cells and the stably Rag1-expressing

HEC293-Rag1 cell line. We first examined neuronal cell survival following transfection with Rag1-shRNA or its negative control, Scr-shRNA. The downregulation of Rag1 by Rag1-shRNA resulted in less in NMDA-induced neuronal cell death than that by Scr-shRNA (Fig. 4C-F). Western blot experiments with whole cell lysates obtained from the HEC293-Rag1 cell line and its control cell line, HEC293-control, were subsequently performed in order to verify the physiological function of Rag1 in the apoptosis signal cascade. The expression of the apoptotic signaling factors Bax, and cleaved caspase-3, 8, and 9 in the HEC293-Rag1 cell line was significantly higher than that in the controls (Fig. 4G). Rap75 and α Tubulin as internal controls in Rag1-overexpressing cell lysates were detected at similar levels to those in control lysates. These findings demonstrated that Rag1 contributed specifically to the NMDA-induced apoptosis signal cascade.

Rag1 is detected in the human GCL

We examined the expression of Rag1 in the human retina using normal adult eyes purchased from Capital Bioscience, Inc. Similarly to our IHC analysis of the mouse retina, Rag1, but not Rag2, was detected in the cytoplasm of RGCs in the human retina (Fig. 5A, B). To determine whether the Rag1 expressed in human retinas had similar function to that in mice, we investigated Rag1 protein homology using NCBI BLAST version 2.2.29. Mouse Rag1 showed a high sequence homology of 90% with its human ortholog (Fig. S1). Taken together, these results suggested that Rag1 participated in the programmed cell death of RGCs in both human and mouse retinas.

Discussion

The intracellular pathways related to cell survival regulate neuronal physiology during embryonic development as well as the pathogenesis of various neurodegenerative disorders. The NF- κ B pathway was discovered in 1986 as a transcription modulator of the light chain of B lymphocyte immunoglobulins [19]. Subsequent studies have shown that NF- κ B is a ubiquitously expressed dimeric transcription factor involved in numerous cellular processes, such as inflammation, differentiation, apoptosis, and oncogenesis. NF- κ B is a dimer composed of members of the Rel family, which includes RelA(p65), RelB, and c-Rel [20]. The NF- κ B family plays important roles in

nervous system development and pathology by influencing neuronal apoptosis, neurite outgrowth, and synaptic plasticity. However, the range of intercellular signals and transduction mechanisms that regulate NF- κ B activity in neurons is broad and complex. Knockout mice have been extensively used to assess different gene components in the NF- κ B pathway. For instance, $p50^{-/-}$ mice exhibited the age-related degeneration of neuronal and non-neuronal cells and defective NF- κ B activation resulted in apoptosis in the striatal neurons in a Huntington disease model [21-23]. Our group also reported that the number of RGCs was significantly lower in $p50^{-/-}$ mice than in $p50^{+/+}$ mice, suggesting a relationship between NF- κ B activity and neuronal apoptosis [9]. Therefore, we searched for a new target related to NF- κ B pathways in neurons.

Rags which comprise Rag1 and Rag2 subtypes, are a group of stable DNA fragments that play a critical role in the development and maturation of lymphocytes [15]. Rags have been detected not only in the immune systems of mammals and amphibians, but also in their nervous systems; low levels of *Rag1* transcripts have been found in the murine CNS in several studies [12-14, 24]. Although the role of the Rag1 locus in the CNS is currently unclear, Rags are known to be regulated by NF- κ B [10]. Based on the above-mentioned findings, we focused on Rag1 as a novel candidate target related to NF- κ B pathways in neurons using $p50^{-/-}$ mice as a model of optic nerve neuropathy. Since no studies have been published on the expression of Rag1 in the visual system, we initially confirmed the presence of Rag1 transcripts in this area and located them in RGCs. In vertebrate embryonic development, the retina and optic nerve originate as outgrowths of the developing brain, and, thus, the retina is considered to be part of the CNS. Furthermore, three-dimensional cultures of mouse embryonic stem cell aggregates have demonstrated the autonomous formation of the optic cup, which develops into the outer and inner layers of the retina structure from brain balls [25]. Glutamate is the major excitatory neurotransmitter of the vertical pathways through the retina, wherein RGCs first express the NMDA glutamate receptors that are typical in the brain [26, 27]. Since the brain and retina have a close relationship in genesis and neurotransmission, it is plausible that Rag1, which has been detected in hippocampus, is also expressed in the retina.

We assessed the precise role of Rag1 in the retina using experiments with $p50^{-/-}$ mice, which

exhibit age-dependent decreases in RGCs. A lack of Rag1 in $p50^{-/-}$ mice diminished the loss of RGC, which was confirmed by several lines of evidence in the present study. These results promoted us to speculate that Rag1 may play a role in the programmed cell death of RGCs. We found that Rag1 was also localized in the nucleus of RGCs in 15-month-old $p50^{-/-}$ mice whose RGC number had already markedly decreased, therefore we proposed that Rag1 may specifically influences apoptotic signaling in the nucleus (Fig. 6A, B).

Many questions still remain regarding the molecular mechanisms involved in Rag1 functions in the retina. However, Rag1 may play a role in RGCs that is entirely distinct from somatic recombination. The evidence for this lies in studies of the molecular structure of the recombinase enzymes themselves; although both Rag1 and Rag2 share several roles, i.e., DNA cleavage and rearrangement of V(D)J recombination, only Rag1 contains the catalytic DNA-binding core of the recombinase [28]. These domains are known to be similar to the active site of several transposases and integrases [29]. Kelch motifs, which mediate the interaction of Rag2 and Rag1, have been observed in numerous proteins [30], and Rag1 may interact with an identified protein via a kelch motif in the retina.

As in the mouse retina, we confirmed the localization of Rag1, but not Rag2, in RGCs in the human retina. The catalytic domains, zinc-finger, recombinase, and RING-finger in the Rag1 molecule appear to be conserved between species (Fig. S1). These results indicated the physiological significance of Rag1 in human RGC survival, similar to that in murine RGCs. We conclude that Rag1 may also be involved in the programmed cell death of RGCs in the human glaucomatous retina. Further studies on the role of Rag1 in RGCs are expected to contribute to the development of preventive and therapeutic treatments for human glaucoma.

Experimental procedures

Animals

All the wild-type ($p50^{+/+}$), heterozygous, and homozygous mice examined in our experiments were littermates of NF- κ Bp50-deficient ($p50^{-/-}$) F8 mice generated by backcrossing with C57BL/6 J mice (CLEA Japan, Inc., Tokyo, Japan). We specifically obtained mice homozygous for the *Nfkb1*^{tm1Bal}

target mutation, which had approximate B6/129-F2 genetic backgrounds, from Jackson Laboratories (Bar Harbor, ME). *p50*^{-/-} mice were crossbred with Rag1-deficient (*Rag1*^{-/-}) mice (a kind donation from Chiba University Graduate School of Medicine) according to previously published protocols[31]. Thus, all mouse strains shared a uniform C57BL/6 genetic background. All genotypes were determined by conventional PCR using isolated DNA from tail biopsy specimens, as previously described [32]. Mice were kept in a specific pathogen-free room at Shinshu University animal facilities in accordance with local guidelines (approval no. 03-28-008).

Western blot analysis

In Western blot analysis, mouse retinas were homogenized and lysed with modified RIPA buffer (50 mM Tris [pH 7.4], 1% NP-40, 0.25% Na-deoxycholic acid, 150 mM NaCl, 1mM Na₃VO₄, and 1 µg/ml each of aprotinin, leupeptin, and pepstatin). Whole retina lysates and whole cell lysates obtained from the control HEK293 cell line and the HEK293-Rag cell line, which stably expresses Rag1 (OriGene Technologies, Inc., Rockville, MD) were heated to 95°C for 10 min and then centrifuged at 15000 rpm for 20 min before storage of supernatants as retinal crude extracts at -30°C. Cell lysates (10 µg) were run on SDS-PAGE (Mini-PROTEAN[®] TGX[™] Precast Gels, Bio-Rad Laboratories, Hercules, California), and a western blot analysis was performed with specific antibodies to Rag1 (Santa Cruz Biotechnology Inc., Santa Cruz, CA), Rag2 (Santa Cruz Biotechnology Inc., Santa Cruz, CA), Bax (TREVIGEN, Gaithersburg, MD), Cleaved Caspase3 (TREVIGEN, Gaithersburg, MD), Cleaved Caspase8 (TREVIGEN, Gaithersburg, MD), Cleaved Caspase9 (Abcam, Cambridge, England), Rap74 (Santa Cruz Biotechnology Inc., Santa Cruz, CA), and αTubulin (MBL Co. Ltd., Nagoya, Aichi, Japan).

RGC quantification

RGCs were quantified histopathologically and by retrograde labeling. The number of cells in the ganglion cell layer (GCL) was counted manually using light microscopy in paraffin sections of the retina (6 µm in thickness) that had been cut through the optic nerve head and ora serrata and stained with hematoxylin and eosin. Cells infiltrating the GCL: phagocytes were excluded. We then

quantified the number of live RGCs in flat-mounted retinas after retrograde labeling. Mice were anaesthetized by the intraperitoneal administration of sodium pentobarbital (150 mg/kg). The skin over the cranium was incised to expose the scalp. The designated point of injection was at a depth of 2 mm from the brain surface, 3 mm behind the bregma in the anteroposterior axis, and 0.5 mm lateral to the midline. A window was drilled and the neurotracer dye Fluoro-Gold (4% solution in saline; Fluorochrome, Denver, CO) was administered (1 μ l at a rate of 0.5 μ l/min) to each hemisphere using a Hamilton syringe. The skin flap was closed following the application of the tracer. Seven days afterwards, mice were euthanized and the retinas were detached as flattened whole mounts in 4% paraformaldehyde PBS. Four standard areas (0.04 mm²) in each retina located 0.1 mm from the optic disc were randomly chosen, and labeled cells were counted by observers blinded to the identity of the mouse.

Intraocular pressure measurement

Intraocular pressure (IOP) was recorded for wild-type, *p50*^{-/-}, *Rag1*^{-/-}, and *p50*^{-/-}*Rag1*^{-/-} mice. Mice were first slightly anesthetized by an intraperitoneal injection of sodium pentobarbital (150 mg/kg). IOP was then determined by trained observers beginning 10 min after the induction of anesthesia using a TonoLab tonometer (TioLat, Helsinki, Finland), as described previously [33].

Immunofluorescence

To examine the expression levels of target molecules, we performed Rag1, Rag2, Brn3a, and Neurofilament 70 kDa (NF70) immunofluorescence experiments on paraffin-embedded mouse and human retina, optic nerve, brain, and bone marrow sections. Paraffin-embedded human retina sections that were purchased from Capital Biosciences, Inc. (Rockville, MD) were first dewaxed and incubated in 1% bovine serum albumin. The sections were then incubated with the appropriate antibodies at 4°C overnight. Regarding primary antibodies, we used a goat polyclonal antibody to Rag2 (1:200, Santa Cruz Biotechnology Inc., Santa Cruz, CA) or Brn3a (1:200, Abcam, Cambridge, England), a rabbit polyclonal antibody to Rag1 (1:200, Santa Cruz Biotechnology), and a mouse

monoclonal antibody to NF70 (1:200, Merck Millipore, Darmstadt, Germany). After being incubated with the secondary antibody of Alexa Fluor 488- or 546-conjugated anti-goat, anti-rabbit, or anti-mouse IgG (1:200, Santa Cruz Biotechnology), respectively, sections were coverslipped with mounting medium and DAPI (VECTASHILD, Vector Laboratory, CA) and visualized using a confocal microscope (Carl Zeiss, Thornwood, NY). Normal rabbit or mouse antiserum was used as a negative control.

RGC purification

Retinal tissues were dissociated to single cell suspensions by the enzymatic degradation of extracellular adhesion proteins maintain structural integrity using Neural Tissue Dissociation kits (MACS Militenyi Biotec, Auburn, CA) according to the manufacturer's recommendations. RGCs were purified by MACS bead assays with mouse CD90.2/Thy1.2 MicroBeads (MACS Militenyi Biotec, Auburn, CA) according to the manufacturer's instructions.

Polymerase chain reaction (PCR)

Total RNA was obtained from mouse tissue, bone marrow, thymus, and RGC samples by Trizol (Invitrogen, Grand Island, NY) extraction following the manufacturer's instructions. Aliquots of 1 μ g total RNA were then reverse transcribed into cDNA using the ImProm-II Reverse Transcription System according to the manufacturer's recommendations (Promega Corporation, Madison, WI). RT-PCR was performed using specific primer sets with an Eppendorf Mastercycler (Eppendorf AG, Hamburg, Germany). The specific primers for mouse *Rag1* and β -*actin* (as the internal control) mRNA were designed using Primer Express software. Specifically, the *Rag1* forward primer was 5'-CCAAGCTGCAGACATTCTAGCACTC-3' and the *Rag1* reverse primer was 5'-GTCGATCCGGAAAATCCTGGCAATG-3'. Triplicates of each sample were tested under the following cycling conditions: 50°C for 2 min, 95°C for 10 min, and 40 cycles of 95°C for 5sec, 55°C for 30sec, and 72°C for 30sec. Nested PCR with RT-PCR products was performed with a primer set for the detection of *Rag1*. In this assay, the *Rag1* forward primer was 5'-GGCCGGGAGGCCTGTGGAGCAAGGTAGC-3' and

the *Rag1* reverse primer was 5'-TGGCAATGAGGTCTGGCCAGGAAGTGACTC-3'.

Electron microscopy

Mice underwent transcardial perfusion with 4% paraformaldehyde following anesthesia by an intraperitoneal injection of sodium pentobarbital (150 mg/kg). The optic nerves were dissected starting 2 mm behind the globe and placed in a fixative (approximately 20 ml of 2% glutaraldehyde and 2% paraformaldehyde in 0.1 M cacodylate buffer) for 12h. They were then post-fixed in 1% osmium tetroxide, dehydrated in ethanol, and embedded in EPOK812 (Okenshoji, Tokyo, Japan). In transmission electron microscopy, ultra-thin sections were cut perpendicularly to the long axis of the optic nerves on an ultramicrotome, stained with uranyl acetate and lead citrate, and examined on a JEM1200EX transmission electron microscope (JEOL, LTD, Tokyo, Japan). Toluidine blue staining was used for light microscopic observation.

Flow cytometry

Purified RGC samples (200 μ l of cell suspension) were incubated with the Muse Annexin V & Dead Cell reagent for 20 min at room temperature. The concentrations of live, early apoptotic, late apoptotic, and dead cells were calculated with the Muse Annexin V & Dead Cell assay (Millipore) according to the manufacturer's directions. This assay was based on the detection of phosphatidylserine on the surface of apoptotic cells.

NMDA injection

An intravitreal NMDA injection was performed as described previously. A total of 1 μ l of 5 mM NMDA solution in 0.01 M phosphate-buffered saline (PBS) was injected into the vitreous of the left eye of each mouse. The right eyes were injected with PBS alone. We enucleated the eyes 48h after the injection and fixed them in 4% paraformaldehyde before dehydration and paraffin embedding. RGC numbers were estimated in transverse sections using the procedures described above.

In vitro assays

That transfection of pRag1.shRNA or its pScr.shRNA control vector (Santa Cruz Biotechnology Inc.) was carried out with FuGENE6 Transfection Reagent (Roche, IN) according to the manufacturer's recommendations with 1 µg of plasmid DNA and 2×10^5 C17.2 cells (DS PHARMA BIOMEDICAL, Osaka, Japan), which were mouse neuronal stem-like cells placed into 24-well tissue culture dishes (MS-0113L plate, SUMITOMO BAKELITE, Tokyo, Japan) on the previous day. Forty-eight hours after being transfected, live cells were counted manually in specific 0.01-mm² areas of each dish. Immediately afterwards, the cells were treated with NMDA (final concentration: 10 nM). Cell survival was assessed 24 hours after NMDA treatment in the same aforementioned areas.

Statistical analysis

Statistical analysis was performed using GraphPad Prism 6 (GraphPad Software Inc., La Jolla, CA). Results were expressed as the mean \pm SD. The statistical significance of differences in mean values between two populations was assessed using the unpaired *t*-test. Groups of 3 or more were analyzed by a one-way ANOVA followed by Tukey's multiple comparison test. A *P* value < 0.05 was considered to be significant.

Acknowledgments

This work was supported by JSPS KAKEN Grant Numbers 23390400 and 24659759.

Author Contributions

T.H, T.H and T.M planned experiments and analyzed data. T.H and T.H performed all experiments and contributed reagents or other essential material. T.H and T.H wrote the paper.

Conflict of Interest

The authors declare that they have no conflict of interest.

References

1 Baeuerle PA & Baltimore D (1988) I kappa B: a specific inhibitor of the NF-kappa B transcription factor, *Science*. **242**,

540-546.

- 2 Mattson MP & Meffert MK (2006) Roles for NF-kappaB in nerve cell survival, plasticity, and disease, *Cell death and differentiation*. **13**, 852-860.
- 3 Sha WC, Liou HC, Tuomanen EI & Baltimore D (1995) Targeted disruption of the p50 subunit of NF-kappa B leads to multifocal defects in immune responses, *Cell*. **80**, 321-330.
- 4 Hoffmann A, Leung TH & Baltimore D (2003) Genetic analysis of NF-kappaB/Rel transcription factors defines functional specificities, *The EMBO journal*. **22**, 5530-5539.
- 5 Fan W & Cooper NG (2009) Glutamate-induced NFkappaB activation in the retina, *Investigative ophthalmology & visual science*. **50**, 917-925.
- 6 Grilli M, Pizzi M, Memo M & Spano P (1996) Neuroprotection by aspirin and sodium salicylate through blockade of NF-kappaB activation, *Science*. **274**, 1383-1385.
- 7 Nakai M, Qin ZH, Chen JF, Wang Y & Chase TN (2000) Kainic acid-induced apoptosis in rat striatum is associated with nuclear factor-kappaB activation, *Journal of neurochemistry*. **74**, 647-658.
- 8 Chen YG, Zhang C, Chiang SK, Wu T & Tso MO (2003) Increased nuclear factor-kappa B p65 immunoreactivity following retinal ischemia and reperfusion injury in mice, *Journal of neuroscience research*. **72**, 125-131.
- 9 Takahashi Y, Katai N, Murata T, Taniguchi SI & Hayashi T (2007) Development of spontaneous optic neuropathy in NF-kappaBetap50-deficient mice: requirement for NF-kappaBetap50 in ganglion cell survival, *Neuropathol Appl Neurobiol*. **33**, 692-705.
- 10 Verkoczy L, Ait-Azzouzene D, Skog P, Martensson A, Lang J, Duong B & Nemazee D (2005) A role for nuclear factor kappa B/rel transcription factors in the regulation of the recombinase activator genes, *Immunity*. **22**, 519-31.
- 11 Mombaerts P, Iacomini J, Johnson RS, Herrup K, Tonegawa S & Papaioannou VE (1992) RAG-1-deficient mice have no mature B and T lymphocytes, *Cell*. **68**, 869-877.
- 12 Chun JJ, Schatz DG, Oettinger MA, Jaenisch R & Baltimore D (1991) The recombination activating gene-1 (RAG-1) transcript is present in the murine central nervous system, *Cell*. **64**, 189-200.
- 13 Feng B, Bulchand S, Yaksi E, Friedrich RW & Jesuthasan S (2005) The recombination activation gene 1 (Rag1) is expressed in a subset of zebrafish olfactory neurons but is not essential for axon targeting or amino acid detection, *BMC Neurosci*. **6**, 46.
- 14 Fang M, Yin Y, Chen H, Hu Z, Davies H & Ling S (2013) Contribution of Rag1 to spatial memory ability in rats, *Behav Brain Res*. **236**, 200-209.
- 15 Oettinger MA, Schatz DG, Gorka C & Baltimore D (1990) RAG-1 and RAG-2, adjacent genes that synergistically activate V(D)J recombination, *Science*. **248**, 1517-1523.
16. Jeon CJ, Strettoi E & Masland RH (1998) The major cell populations of the mouse retina, *The Journal of neuroscience : the official journal of the Society for Neuroscience*. **18**, 8936-8946.
- 17 Galindo-Romero C, Aviles-Trigueros M, Jimenez-Lopez M, Valiente-Soriano FJ, Salinas-Navarro M, Nadal-Nicolas F, Villegas-Perez MP, Vidal-Sanz M & Agudo-Barriuso M (2011) Axotomy-induced retinal ganglion cell death in adult mice: quantitative and topographic time course analyses, *Experimental eye research*. **92**, 377-387.
- 18 Ullian EM, Barkis WB, Chen S, Diamond JS & Barres BA (2004) Invulnerability of retinal ganglion cells to NMDA excitotoxicity, *Molecular and cellular neurosciences*. **26**, 544-557.
- 19 Sen R & Baltimore D (1986) Multiple nuclear factors interact with the immunoglobulin enhancer sequences, *Cell*. **46**, 705-716.

- 20 Huxford T, Malek S & Ghosh G (1999) Structure and mechanism in NF-kappa B/I kappa B signaling, *Cold Spring Harbor symposia on quantitative biology*. **64**, 533-540.
- 21 Lu ZY, Yu SP, Wei JF & Wei L (2006) Age-related neural degeneration in nuclear-factor kappaB p50 knockout mice, *Neuroscience*. **139**, 965-978.
- 22 Yu Z, Zhou D, Bruce-Keller AJ, Kindy MS & Mattson MP (1999) Lack of the p50 subunit of nuclear factor-kappaB increases the vulnerability of hippocampal neurons to excitotoxic injury, *The Journal of neuroscience : the official journal of the Society for Neuroscience*. **19**, 8856-8865.
- 23 Yu Z, Zhou D, Cheng G & Mattson MP (2000) Neuroprotective role for the p50 subunit of NF-kappaB in an experimental model of Huntington's disease, *Journal of molecular neuroscience : MN*. **15**, 31-44.
- 24 Wang X, Su H & Bradley A (2002) Molecular mechanisms governing Pcdh-gamma gene expression: evidence for a multiple promoter and cis-alternative splicing model, *Genes & development*. **16**, 1890-1905.
- 25 Eiraku M, Takata N, Ishibashi H, Kawada M, Sakakura E, Okuda S, Sekiguchi K, Adachi T & Sasai Y (2011) Self-organizing optic-cup morphogenesis in three-dimensional culture, *Nature*. **472**, 51-56.
- 26 Massey SC & Miller RF (1988) Glutamate receptors of ganglion cells in the rabbit retina: evidence for glutamate as a bipolar cell transmitter, *The Journal of physiology*. **405**, 635-655.
- 27 Yazejian B & Fain GL (1992) Excitatory amino acid receptors on isolated retinal ganglion cells from the goldfish, *Journal of neurophysiology*. **67**, 94-107.
- 28 Fugmann SD, Lee AI, Shockett PE, Villey IJ & Schatz DG (2000) The RAG proteins and V(D)J recombination: complexes, ends, and transposition, *Annual review of immunology*. **18**, 495-527.
- 29 Zhou L, Mitra R, Atkinson PW, Hickman AB, Dyda F & Craig NL (2004) Transposition of hAT elements links transposable elements and V(D)J recombination, *Nature*. **432**, 995-1001.
- 30 Prag S & Adams JC (2003) Molecular phylogeny of the kelch-repeat superfamily reveals an expansion of BTB/kelch proteins in animals, *BMC bioinformatics*. **4**, 42.
- 31 Ip CW, Kroner A, Bendszus M, Leder C, Kobsar I, Fischer S, Wiendl H, Nave KA & Martini R (2006) Immune cells contribute to myelin degeneration and axonopathic changes in mice overexpressing proteolipid protein in oligodendrocytes, *The Journal of neuroscience : the official journal of the Society for Neuroscience*. **26**, 8206-8216.
- 32 Han S, Zheng B, Schatz DG, Spanopoulou E & Kelsoe G (1996) Neoteny in lymphocytes: Rag1 and Rag2 expression in germinal center B cells, *Science*. **274**, 2094-2097.
- 33 Qiu Y, Yang H & Lei B (2013) Effects of Three Commonly Used Anesthetics on Intraocular Pressure in Mouse, *Current eye research*. **39**, 365-369.

Supporting information

Fig. S1. Homology between mouse *Rag1* and human *RAG1* at the amino acid level.

Figure legends

Fig. 1. Rag1 expression in RGCs. (A) Immunofluorescent labeling of Rags. Isolated retina (upper panel), bone marrow (lower left), and brain (lower right) specimens from 6-month-old *p50^{+/+}* mice labeled with antibodies to Rag1, Rag2, and DAPI. Rag1 was detected in the ganglion cell layer,

whereas Rag2 was not. Both Rag1 and Rag2 were present in lymphocytes. Only Rag1 was visible in the hippocampus. Scale bar = 50 μ m. H.E., hematoxylin and eosin staining; DG, dentate gyrus; CA, hippocampal cornu ammonis region. (B) Isolated optic nerve specimens from 6-month-old $p50^{+/+}$ mice labeled with antibodies to Rag1, Rag2, and DAPI. Neither Rag1 nor Rag2 were detectable. Scale bar (white) = 100 μ m; Scale bar (black) = 200 μ m. H.E., hematoxylin and eosin staining. (C) Immunohistochemical analysis of DAPI, Brn3a, and Rag1 in retinal sections of 6-month-old $p50^{+/+}$ mice. Rag1 was detected in the cytoplasm of Brn3a-positive cells (arrows). An analysis of normal rabbit IgG revealed no significant findings. Scale bar = 20 μ m. (D) Western blot analysis of Rag1 in retina crude extracts derived from 6-month-old $p50^{+/+}$ and $p50^{-/-}$ mice, and crude extracts prepared from bone marrow and the thymus obtained from $p50^{+/+}$ mice. Rag1 (119 kDa) was detected in both groups as well as α Tubulin (50 kDa), whereas Rag2 (59 kDa) was not. (E) Rag1 levels were significantly higher in $p50^{-/-}$ mice than in $p50^{+/+}$ mice. The student's *t*-test. $*P < 0.05$. (n = 8 per group). (F) *Rag1* mRNA expression in the retinas of 6-month-old $p50^{+/+}$ mice analyzed by RT-PCR. Although *Rag1* mRNA was faintly detected in RGCs, its expression in purified RGCs was clearly visible using nested PCR. *Rag1* mRNA was not detected in retinal cells, apart from RGCs, as indicated in the other lanes. *Rag1* mRNA was clearly detected in bone marrow and the thymus obtained from $p50^{+/+}$ mice. GCL, ganglion cell layer; IPL, inner plexiform layer; N. IgG, normal IgG; M, molecular weight marker; RGCs, retinal ganglion cells; BM, bone marrow; Thy., thymus.

Fig. 2. Effects of Rag1 knockdown in $p50^{-/-}$ mice. (A) and (B) Age-dependent reduction in GCL cell number in $p50^{-/-}$ mice. (A) Histological examination of the retina in 6- and 15-month-old mice showed that the number of cells in the GCL was reduced in $p50^{-/-}$ mice as compared with $p50^{+/+}$ mice. Scale bar = 50 μ m. (B) The quantification of GCL cell number also showed that in both 6- and 15-month-old $p50^{-/-}$ mice, the number of cells was significantly decreased as compared with $p50^{+/+}$ mice. (n = 10 per group). $***P < 0.001$. (C) and (D) H.E. staining of retinal preparations (C) and quantification of cell numbers in the GCL in 6-month-old $p50^{+/+}$, $p50^{-/-}$, $p50^{-/-}Rag1^{-/-}$, and

Rag1^{-/-} mice (D). The GCL cell number was significantly lower in *p50*^{-/-} mice than in *p50*^{+/+} mice; however no significant differences were observed between *p50*^{+/+} and *p50*^{-/-}*Rag1*^{-/-} or *Rag1*^{-/-} mice (n = 10-12 per group). Brn3-positive cells, which indicated RGCs, are represented in white dotted-line boxes. Scale bar = 50 μm. (E) Immunohistochemical analysis of DAPI, Brn3a, and *Rag1* in retina sections and (F) quantification of Brn3a-positive cell numbers of the GCL in 6-month-old *p50*^{+/+}, *p50*^{-/-}, *p50*^{-/-}*Rag1*^{-/-}, and *Rag1*^{-/-} mice. The Brn3a-positive cell number was significantly lower in *p50*^{-/-} mice than in *p50*^{+/+} mice, whereas no significant differences were observed between *p50*^{+/+} and *p50*^{-/-}*Rag1*^{-/-} or *Rag1*^{-/-} mice. The quantification of cells other than Brn3a-positive cells in the GCL revealed no significant differences among the four groups. (n = 10 per group). **P* < 0.05; ***P* < 0.01; ****P* < 0.001. (G) Fluorescence micrographs of flat-mounted retinal preparations 7 days after the injection of Fluoro-Gold into the superior colliculus of 6-month-old *p50*^{+/+}, *p50*^{-/-}, *p50*^{-/-}*Rag1*^{-/-}, and *Rag1*^{-/-} mice. Left: Scale bar = 500 μm; Right: Scale bar = 50 μm. (H) The quantification of Fluoro-Gold-labeled RGCs revealed loss of cells was significantly greater in *p50*^{-/-} mice than in *p50*^{+/+} mice, whereas no significant differences were observed in RGC numbers between *p50*^{+/+} and *p50*^{-/-}*Rag1*^{-/-} or *Rag1*^{-/-} mice (n = 6 per group). (I) The distribution of live, early apoptotic, late apoptotic, and dead cells was measured by flow cytometry using purified RGC samples from *p50*^{+/+}, *p50*^{-/-}, *p50*^{-/-}*Rag1*^{-/-}, and *Rag1*^{-/-} mice. (J) The quantification of the total apoptotic cell ratio, which was calculated as the total amount of late and early apoptotic cell ratios, revealed that this ratio was significantly higher in *p50*^{-/-} mice than in *p50*^{+/+}, *p50*^{-/-}*Rag1*^{-/-}, and *Rag1*^{-/-} mice (n = 8 per group). A one-way ANOVA followed by Tukey's post hoc test. **P* < 0.05; ***P* < 0.01; ****P* < 0.001. GCL, ganglion cell layer; INL, inner nucleus layer; ONL, outer nucleus layer; NS, not significant.

Fig. 3. A *Rag1* deficiency was not related to the optic nerve cross-sectional area or axon density, but appeared to ameliorate axon degeneration. (A) Photomicrographs of toluidine blue-stained optic nerve sections taken from 6-month-old *p50*^{+/+}, *p50*^{-/-}, *p50*^{-/-}*Rag1*^{-/-}, and *Rag1*^{-/-} mice. Scale bars = 100 μm. (B) Measurement of optic nerve cross-sectional areas in mice. No significant differences

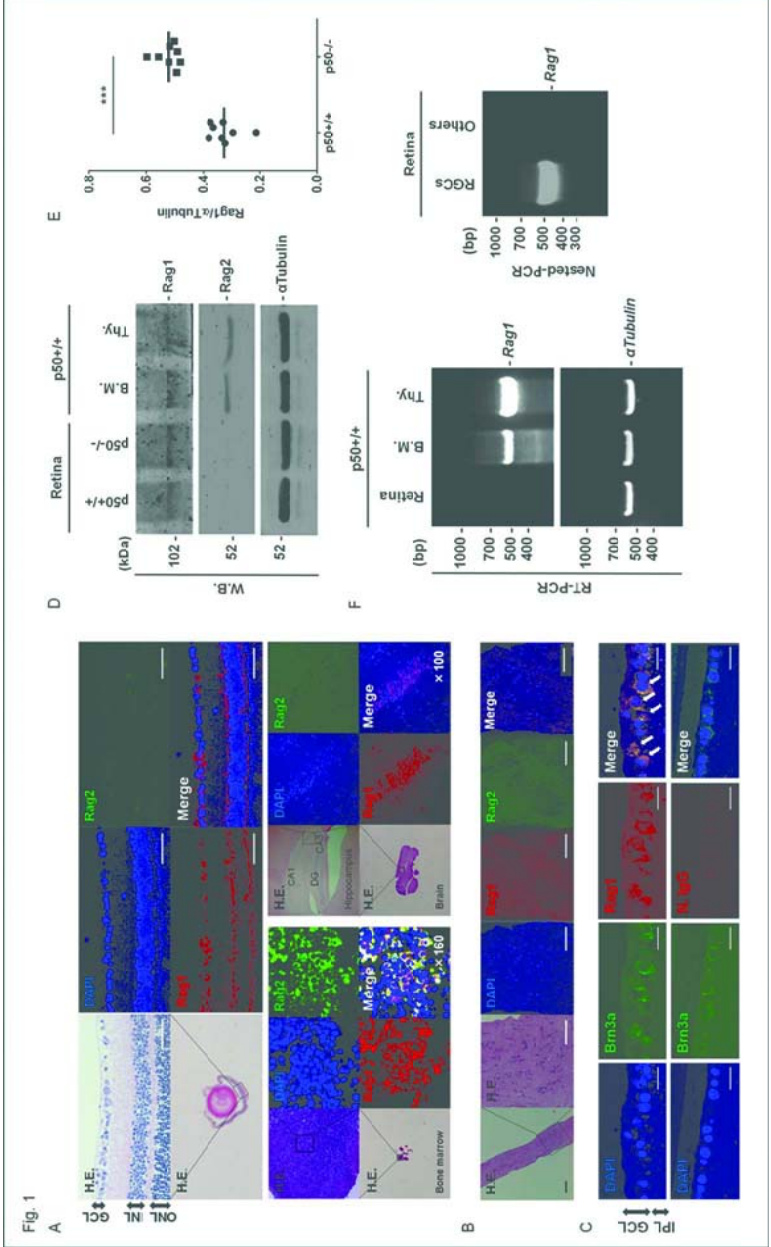
were noted. (n = 6 per group). (C) Electron microscopic photomicrographs of optic nerve sections taken from 6-month-old $p50^{+/+}$, $p50^{-/-}$, $p50^{-/-} Rag1^{-/-}$, and $Rag1^{-/-}$ mice. Scale bars = 5 μ m. Inset: high-magnification image of axon degeneration. (D) The quantification of RGC axon densities. No significant differences were detected. (n = 6 per group). (E) The quantification of degenerating axons revealed there were significantly more in $p50^{-/-}$ mice than $p50^{+/+}$, $p50^{-/-} Rag1^{-/-}$, and $Rag1^{-/-}$ mice. (n = 6 per group). $*P < 0.05$; $***P < 0.001$. (F) Intraocular pressure (IOP) measurement of eyes obtained from 6-month-old $p50^{+/+}$, $p50^{-/-}$, $p50^{-/-} Rag1^{-/-}$, and $Rag1^{-/-}$ mice. (n = 10 per group). No significant differences were observed in IOP among the 4 groups. (G) Photomicrographs of hematoxylin and eosin-stained anterior segments of the eyeball collected from 6-month-old $p50^{+/+}$, $p50^{-/-}$, $p50^{-/-} Rag1^{-/-}$, and $Rag1^{-/-}$ mice. Morphological changes, including angle closure, were not observed in any mouse group. Scale bars = 200 μ m.

Fig. 4. Silencing Rag1 reduces cell death. (A) and (B) H.E. staining of retina preparations (A) and quantification of cell numbers in the GCL of 6-month-old $p50^{+/+}$, $p50^{-/-}$, $p50^{-/-} Rag1^{-/-}$, and $Rag1^{-/-}$ mice with or without the NMDA treatment (n = 9 per group) (B). Scale bar = 50 μ m. No significant differences were observed in the number of GCL cells among the 4 test groups without the NMDA treatment. However, the number of cells in the GCL was significantly lower in $p50^{-/-}$ mice than in $p50^{+/+}$, $p50^{-/-} Rag1^{-/-}$, and $Rag1^{-/-}$ mice after the NMDA treatment. A one-way ANOVA followed by Tukey's post hoc test. $*P < 0.05$. (C) C17.2 cells that were transfected with pRag1.shRNA or its control, pScr.shRNA were treated with NMDA (final concentration: 10 nM) 48 hours afterwards. (D) Immunofluorescence examination of C17.2 cells transfected with pRag1.shRNA or pScr.shRNA 48 hours after the NMDA treatment. (E) The fluorescence intensity (arbitrary units) of Rag1 in C17.2 cells transfected with pRag1.shRNA or pScr.shRNA was significantly lower than that in controls. The student's *t*-test. $*P < 0.05$. (F) Living C17.2 cells (%) over 72 hours of monitoring. The results of 4 replicate wells are expressed as the mean \pm SD percentage culture/time point. The student's *t*-test. $*P < 0.05$. NS, not significant. (G) Western blot analysis for indicated proteins, Rag1 (119 kDa), Bax (21 kDa), Caspase3 (31 kDa, 17 kDa) Caspase8 (55 kDa, 18 kDa), Caspase9

(46 kDa, 38 kDa), Rap74 (74 kDa), α Tubulin (50 kDa), in lysates prepared from HEK293 cells and HEK293 Rag1 expressing cells.

Fig. 5. Rag1 expression in tissue sections obtained from the human retina. (A) H.E. staining (upper panel) and IHC analysis (lower panel) of DAPI, Rag1, and NF70 in human retinal preparations. Rag1 was detected in the GCL, whereas normal rabbit (red) and mouse (green) IgG were not. Scale bar (black) = 100 μ m; Scale bar (white) = 50 μ m. (B) H.E. staining and IHC analysis of DAPI and Rag2 in human retina preparations. Similar to mice retina, Rag2 was not detected in the GCL. Scale bars = 50 μ m.

Fig. 6. (A) Immunohistochemical analysis of DAPI and Rag1 in retina sections from 15-month-old $p50^{-/-}$ mice. Rag1 was detected in the nucleus. Scale bar = 10 μ m. The quantification of Rag1-positive cell number in the GCL showed that, the number of cells was significantly lower in 15-month-old $p50^{-/-}$ mice than in 6-month-old $p50^{-/-}$ mice. However, the number of intranuclear Rag1-positive cells was significantly higher in 15-month-old $p50^{-/-}$ mice than in 6-month-old $p50^{-/-}$ mice. The number of Rag1-negative cells in GCL, which implicated amacrine cells and others, was similar between the two groups. (n = 10 per group). (B) Signal cascade of cell death mediated by Rag1 in p50-deficient mouse. A recent study demonstrated that the binding site of the hetero dimer p50-RelA (p65) could also be occupied by the homo dimer p50-p50, and may function as a repressor to regulate the role of p50-RelA (p65) as a transcription factor essential for neuronal responses. In p50-deficient neuronal cells, the c-Rel- RelA (p65) hetero dimer markedly induced *Rag1* gene activation as a transcription factor. Rag1 may play a role in neuronal cell death signaling as a nuclear mediator. The cell death factors, Bax and cleaved caspase-3, 8, and 9 were also clearly detected in Rag1-expressing cells.



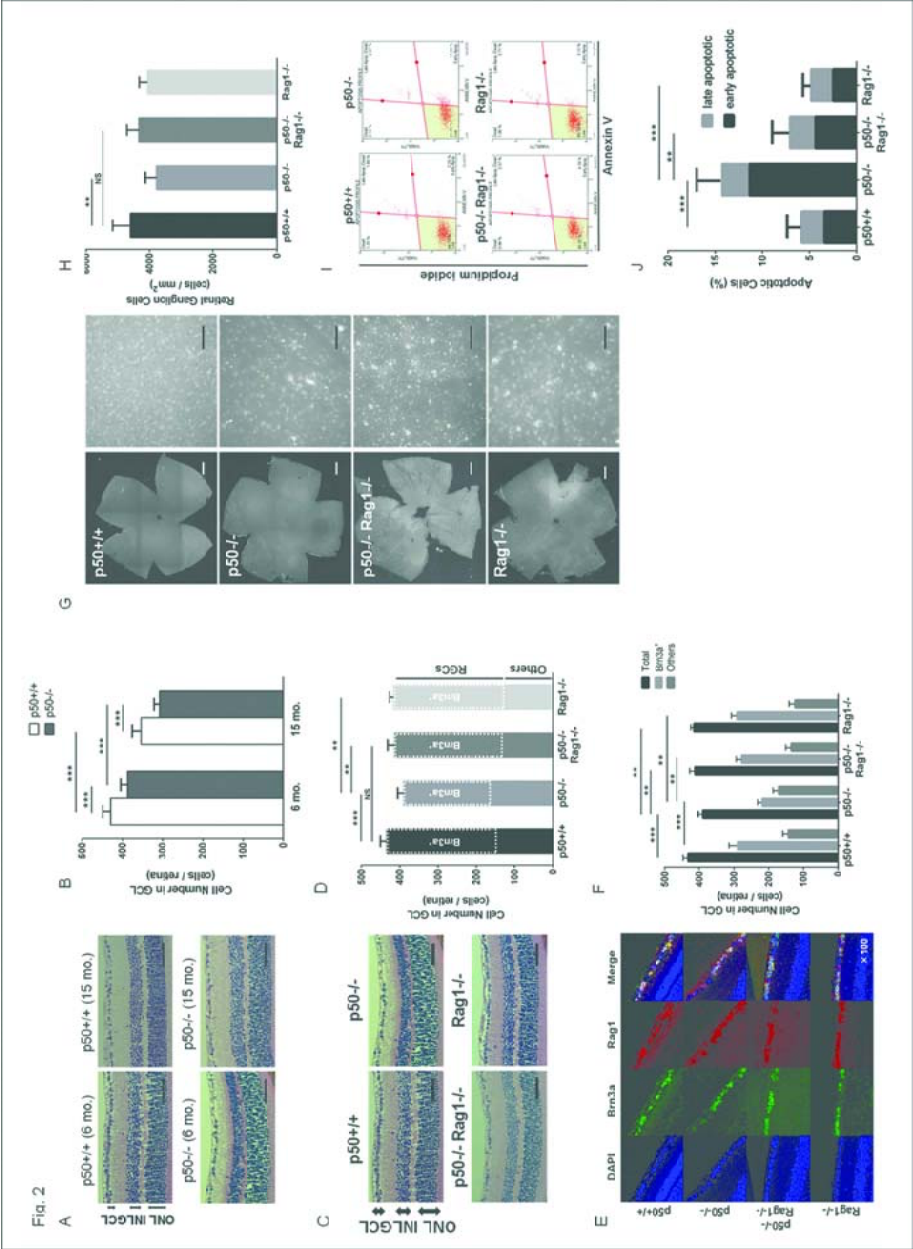


Fig. 3

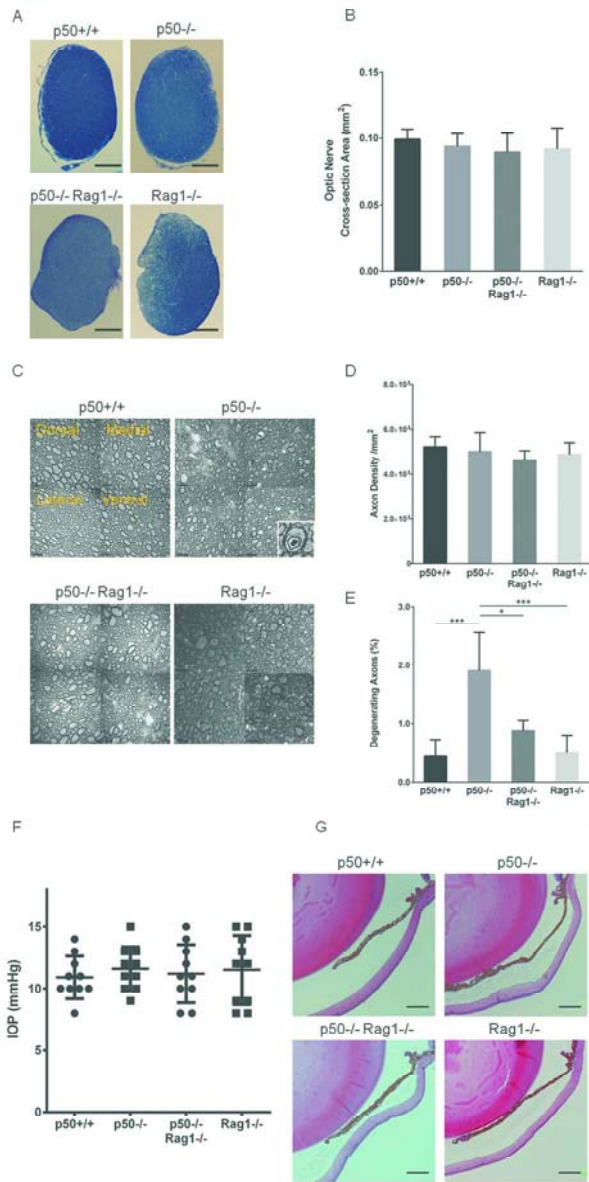
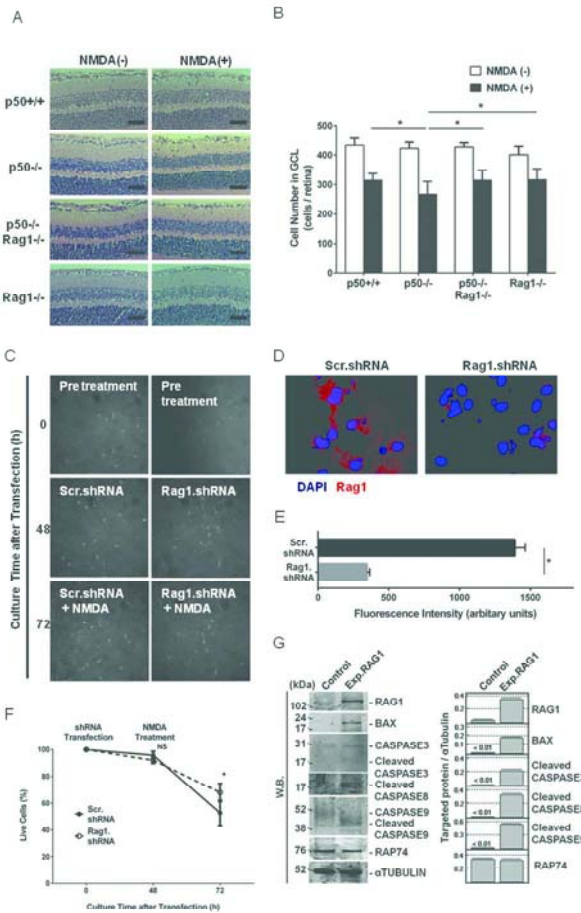


Fig. 4



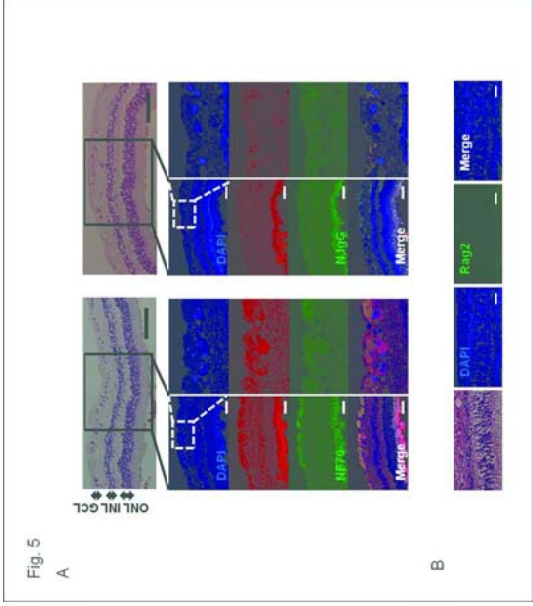
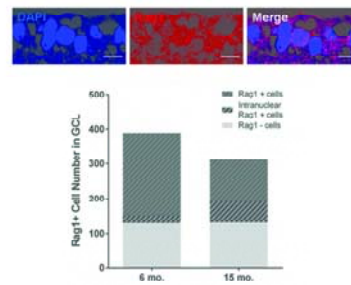
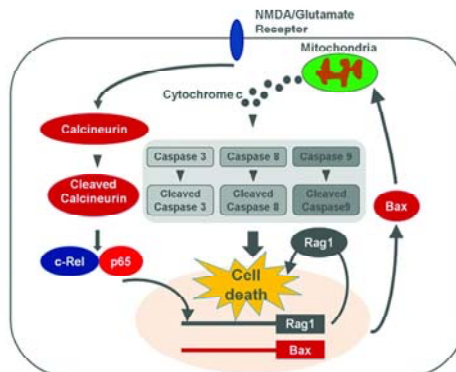


Fig. 6

A



B



Physiological significance of Rag1 in neuronal death, especially optic neuropathy

Takao Hirano, Toshinori Murata, Takuma Hayashi








Fig. S1. Homology between mouse Rag1 and human RAG1 at the amino acid level. **A.** Genes identified as putative homologs of one another during the construction of HomoloGene. **B.** Protein homology between mouse and human Rag1 as assessed by NCBI BLAST version 2.2.29. Mouse Rag1 showed high homology with its human ortholog, with 90% sequence identity. Query and Subject show amino acids for the mouse and human, respectively. The middle section indicates identical regions.

A.

HomoloGene:387. Gene conserved in Euteleostomi

Genes

Genes identified as putative homologs of one another during the construction of HomoloGene.

-  RAG1, *H.sapiens*
recombination activating gene 1
-  RAG1, *P.troglodytes*
recombination activating gene 1
-  RAG1, *M.mulatta*
recombination activating gene 1
-  RAG1, *C.lupus*
recombination activating gene 1
-  RAG1, *B.taurus*
recombination activating gene 1
-  Rag1, *M.musculus*
recombination activating gene 1
-  Rag1, *R.norvegicus*
recombination activating gene 1
-  RAG1, *G.gallus*
recombination activating gene 1
-  rag1, *X.tropicalis*
recombination activating gene 1
-  rag1, *D.erio*
recombination activating gene 1

Protein Alignments

Protein multiple alignment, pairwise similarity scores and evolutionary distances.

Show Multiple Alignment

Show Pairwise Alignment Scores

Pairwise alignments generated using BLAST

Regenerate Alignments











NP_033045.2 (M.musculus)

NP_000439.1 (H.sapiens)

Blast





Proteins

Proteins used in sequence comparisons and their conserved domain architectures.

-  NP_000439.1
1043 aa
-  XP_001154240.1
1043 aa
-  XP_001084631.1
1043 aa
-  XP_540538.1
1043 aa
-  XP_005216456.1
1062 aa
-  NP_033045.2
1040 aa
-  NP_445920.1
1040 aa
-  NP_001026359.1
1041 aa
-  XP_002937338.1
1046 aa
-  NP_571464.1
1057 aa

Conserved Domains

Conserved Domains from CDD found in protein sequences by rpsblast searching.

- zf-RAG1 (pfam10426)
 -  Recombination-activating protein 1 zinc-finger domain.
- RAG1 (pfam12940)
 -  Recombination-activation protein 1 (RAG1).
- zf-C3HC4_2 (pfam13923)
 -  Zinc finger, C3HC4 type (RING finger).
- RING (c17238)
 -  RING-finger (Really Interesting New Gene) domain, a specialized type of Zn-finger of 40 to 60 residues that binds two atoms of zinc; defined by the 'cross-brace' motif C-X2-C-X(9-39)-C-X(1-3)-H-X(2-3)-(N/C/H)-X2-C-X(4-48)-C-X2-C; probably ...

B.

NCBI/BLAST/blastp suite 2sequences/ Formatting Results - 3C2HWAC1114

[Edit and Resubmit](#) [Save Search Strategies](#) [Formatting options](#) [Download](#)[YouTube](#) [How to read this page](#) [Blast report description](#)

Blast 2 sequences

gil133778933 (1040 letters)

RID [3C2HWAC1114](#) (Expires on 10 10 12:08 pm)
Query ID [gil133778933|ref|NP_033045.2|](#)
Description V(D)J recombination-activating protein 1 [Mus musculus]
Molecule type amino acid
Query Length 1040

Subject ID [gil4557841|ref|NP_000439.1|](#)
Description V(D)J recombination-activating protein 1 [Homo sapiens]
Molecule type amino acid
Subject Length 1043
Program BLASTP 2.2.30+ [Citation](#)

Other reports: [Search Summary](#) [Taxonomy reports](#) [Multiple alignment](#)[Dot Matrix View](#)[Descriptions](#)

Sequences producing significant alignments:

Select [All](#) [None](#) Selected: 0[Alignments](#) [Download](#) [GenPept](#) [Graphics](#) [Multiple alignment](#)

	Description	Max score	Total score	Query cover	E value	Ident	Accession
<input type="checkbox"/>	V(D)J recombination-activating protein 1 [Homo sapiens]	1943	1943	100%	0.0	90%	NP_000439.1

[Alignments](#)[Download](#) [GenPept](#) [Graphics](#)[Next](#) [Previous](#) [Descriptions](#)

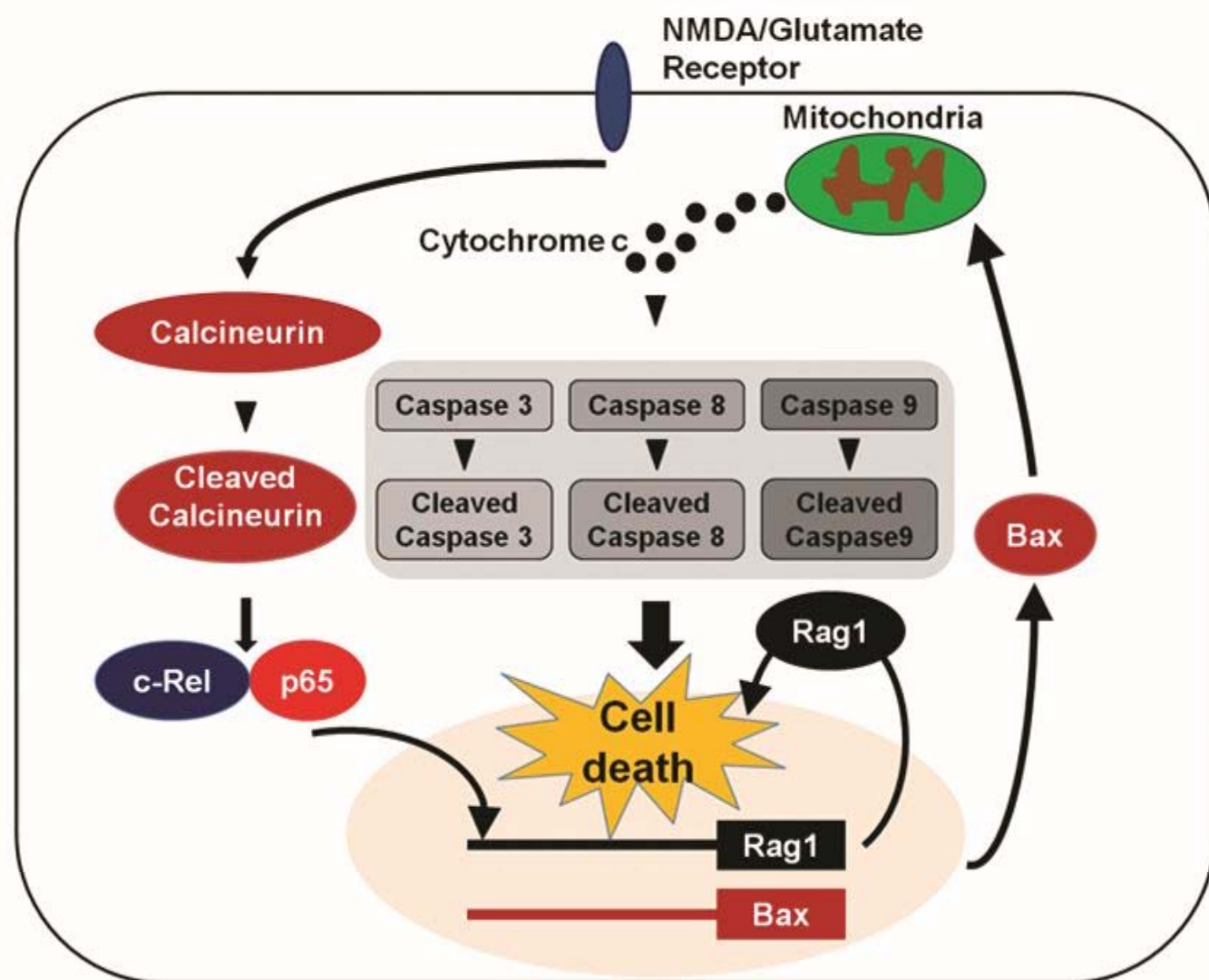
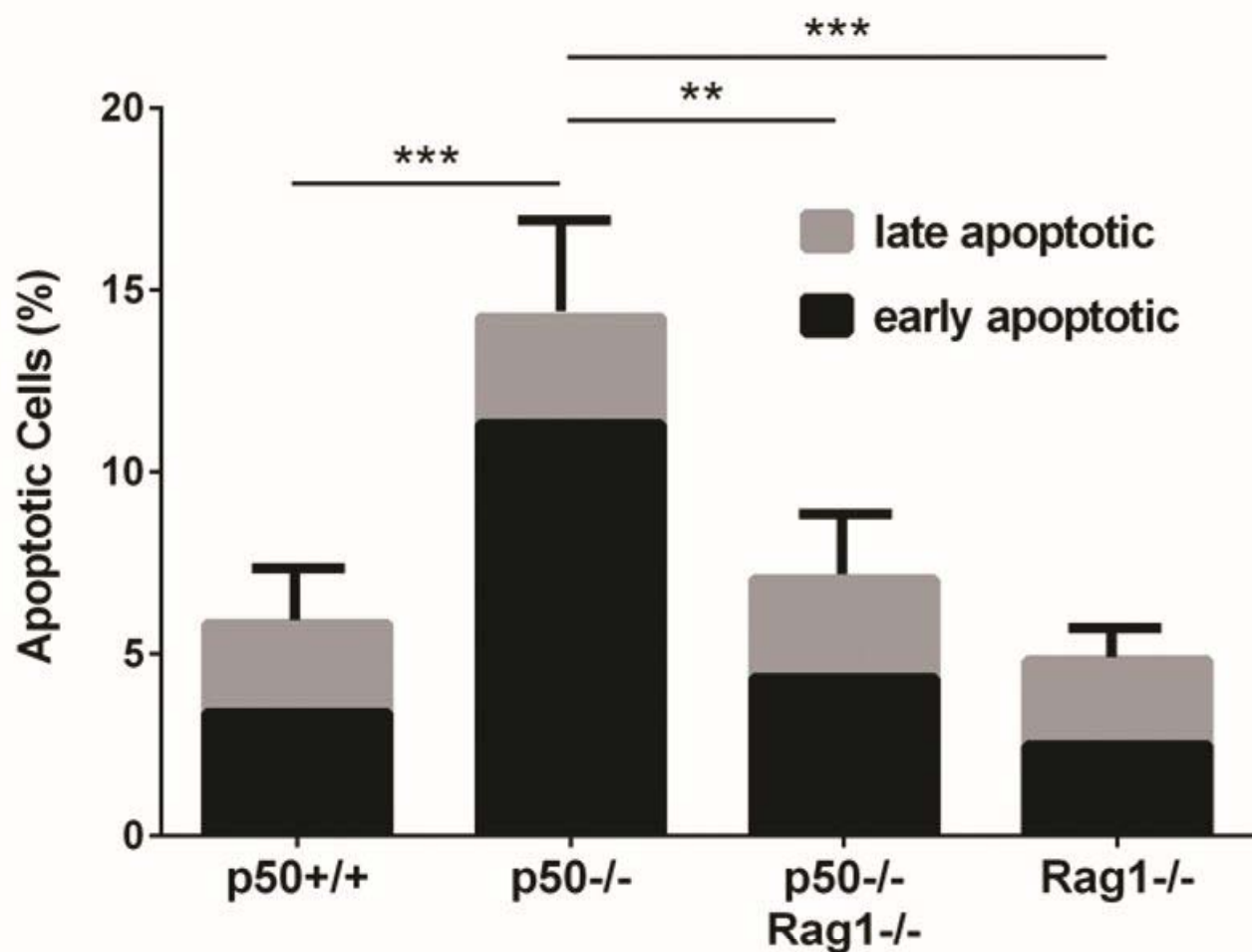
V(D)J recombination-activating protein 1 [Homo sapiens]

Sequence ID: [ref|NP_000439.1|](#) Length: 1043 Number of Matches: 1[See 1 more title\(s\)](#)

Range 1: 1 to 1043			GenPept	Graphics			Next Match	Previous Match
Score	Expect	Method	Identities		Positives	Gaps		
1943 bits(5033)	0.0		Compositional matrix adjust.		934/1043(90%)	984/1043(94%)	3/1043(0%)	
Query	1	MAAQLPOTLSPGAPDEIQHPQIKFSEWKKFLFRVRSFEKAPPEAQKEK-DSSEGRPYLE						59
Sbjct	1	MAAS P TL SSAPDEIQHP IKFSEWKKFLFRVRSFEK PEEAQKEK DS EGK LE						60
Query	60	QSPVVEKPGGNSIITLCRAKLHFKFSSKKFHADGKSSDAVHQARLRHFCRIGNRFS						119
Sbjct	61	OSP V +K GO + TO LE HRFSSKKFH + K+ KA+HQA LRH CRICGN F++						120
Query	120	DGHSRRYPVHGPDVDAKTSLSFRKKEKRVTSWPDLIARIFRIDVKADVDSIHPTFCHDCW						179
Sbjct	121	D H+RRYPVHGPDVDTLGLLRKKERATSWPDLIAKVRIDVKADVDSIHPTFCHNCW						180
Query	180	SIMHRKFSSSHSVOYFFRKVTVEWHPTPSCDICFTAHRLKRRKHPQNVQLSKKLKTVL						239
Sbjct	181	SIMHRKFSS+ +YFFR VT+EWHPHTPSCDIC TA RGLKRR QPN+QLSKKLKTVL						240
Query	240	NHArdrkrktqar--VSSKEVLKKISNCKIHLSTKLLAVDFFAHFVKISQCICEHIL						297
Sbjct	241	+ AR+ R+++ +A+ +SSK+V+K+I+NCCKIHLSTKLLAVDFF HFVKISQCICEHIL						300
Query	298	ADPVETSCKHLFCRICILACLKVMGSCYCPSCRYPCFFTDLESFVKSFILNLSIMVKCPA						357
Sbjct	301	ADPVET+CKH+FCR+CILRCLKVMGSCYCPSCRYPCFFTDLESFVKSF+L+LNSIMVKCPA						360
Query	358	QDCNEEVSLEKYNHHVSSHESKETLVHINKGGRPRQHLLSLTRRAQKRLRELKIQVKE						417
Sbjct	361	KECNEEVSLEKYNHHSSHESKEIFVHINKGGRPRQHLLSLTRRAQKRLRELKIQVKA						420
Query	418	FADKEEGGDVAVCLTLFLALARNRHRQADELAIMQGGSGLOPAVCLAIRVNTFLS						477
Sbjct	421	FADKEEGGDVAVCLTLFLALARNRHRQADELAIMQGGSGLOPAVCLAIRVNTFLS						480
Query	478	CQYHKMYRTVKAITGRQIFQPLHALRNAEKVLLPGYHFFWQPFPLKNVSSSTDVGIIDG						537
Sbjct	481	CQYHKMYRTVKAITGRQIFQPLHALRNAEKVLLPGYHFFWQPFPLKNVSSSTDVGIIDG						540
Query	538	LSGLASSVDEYFVDTIARRFRYDSALVSALMDMEEDILEGMRSDQLDDYLNPGFTVVVKE						597
Sbjct	541	LSGL+SSVD+YFVDTIARRFRYDSALVSALMDMEEDILEGMRSDQLDDYLNPGFTVVVKE						600
Query	598	SCDGMGDSVSEKHGSGPAVPEKAVRFSFTVMRITIEHGSQNVKVFEEPKNSLOCRPLCL						657
Sbjct	601	SCDGMGDSVSEKHGSGPVPEKAVRFSFTIMKITHSSQNVKVFEEPKNSLOCRPLCL						660
Query	658	MLADESDHETLTAILSPLIAERAMKSSSELTLEMGGIPRTFKFIFRGTGYDEKLVRVEEG						717
Sbjct	661	MLADESDHETLTAILSPLIAERAMKSSSELTLEMGGILRTFKFIFRGTGYDEKLVRVEEG						720
Query	718	LEASGSVYICTLCDTTRLEASQNLVFSITRSHAENLQRYEVRNSNPFYHESVEELDRVK						777
Sbjct	721	LEASGSVYICTLCD TRLASQNLVFSITRSHAENL+RYEVRNSNPFYHESVEELDRVK						780
Query	778	GVSARKPIETVPSIDALHCDIGNAAEFYKIFQLEIGEYVYKHPNASKEERKRQATLDRHL						837
Sbjct	781	GVSARKPIETVPSIDALHCDIGNAAEFYKIFQLEIGEYVYKHPNASKEERKRQATLDRHL						840
Query	838	RKRMNLKPIRMINGNFARKIMTQETVDVAVCELIPSEERHEALREIMDLYLKMFPVWRSSC						897
Sbjct	841	RKRMNLKPIRMINGNFARKIMTQETVDVAVCELIPSEERHEALREIMDLYLKMFPVWRSSC						900
Query	898	PAKECPESLCQYFSNQRFAELLSTFKRYRYEGKITNYFHKTLAHVPEIIEPDGSGIGAWA						957
Sbjct	901	PAKECPESLCQYFSNQRFAELLSTFKRYRYEGKITNYFHKTLAHVPEIIEPDGSGIGAWA						960
Query	958	SEGNESGNLFRFRKMNARQSKCYEMEDVLKHHWLYTSKYLOKFMNAHNALKSSGFTMN						1017
Sbjct	961	SEGNESGNLFRFRKMNARQSKCYEMEDVLKHHWLYTSKYLOKFMNAHNALKSSGFTMN						1020
Query	1018	SKETLGDPLGIEDSLESQDSMEF 1040						
Sbjct	1021	+ +LGDPLGIEDSLESQDSMEF 1043						

Related Information

[Gene](#) - associated gene details
[UniGene](#) - clustered expressed sequence
[tags](#)
[Map Viewer](#) - aligned genomic context
[Identical Proteins](#) - Proteins identical to the subject



a short abstract

Although the transcription factor NF- κ B is known to regulate cell death and survival, its precise role in cell death within the central nervous system remains unknown. The result of the present study indicated that Rag1 played a role in optic neuropathy as a pro-apoptotic candidate in NF- κ Bp50-deficient mice. This result may lead to new therapeutic targets in optic neuropathy.

(59 words)